unc-68 Encodes a Ryanodine Receptor Involved in Regulating C. elegans Body-Wall Muscle Contraction

Ed B. Maryon, Roberto Coronado,* and Philip Anderson

Department of Genetics, and Department of Physiology, *University of Wisconsin, Madison, Wisconsin 53706

Abstract. Striated muscle contraction is elicited by the release of stored calcium ions through ryanodine receptor channels in the sarcoplasmic reticulum. *ryr-1* is a *C. elegans* ryanodine receptor homologue that is expressed in body-wall muscle cells used for locomotion. Using genetic methods, we show that *ryr-1* is the previously identified locus *unc-68*. First, transposon-induced deletions within *ryr-1* are alleles of *unc-68*. Second, transformation of *unc-68* mutants with *ryr-1* genomic DNA results in rescue of the Unc phenotype. *unc-68* mutants move poorly, exhibiting an incomplete flaccid paralysis, yet have normal muscle ultrastructure. The mutants are insensitive to the paralytic effects of ryanodine, and lack detectable ryanodine-binding activity. The Unc-68 phenotype suggests that ryanodine receptors are not essential for excitation-contraction coupling in nematodes, but act to amplify a (calcium) signal that is sufficient for contraction.

INTRACELLULAR calcium (Ca^{2+}) channels play a key role in regulating muscle contraction. During excitation-contraction coupling (E-C coupling) in striated muscle, two classes of Ca^{2+} channels act sequentially to cause the release of Ca^{2+} ions stored within the sarcoplasmic reticulum (SR)[1] (Caterall, 1991). Cholinergic excitation opens voltage-gated Ca^{2+} channels in the plasma membrane, which in turn cause voltage-insensitive channels in the SR to flood the cell with Ca^{2+} ions, thus eliciting sarcomere contraction (Coronado et al., 1994; McPherson and Campbell, 1993a; Meissner, 1994). These high conductance calcium release channels in the SR are termed ryanodine receptors (RyRs) because of their specific, high affinity interaction with the plant alkaloid ryanodine (Fill and Coronado, 1988). Ryanodine locks the channels open in a submaximal conductance state, causing a steady leak of Ca^{2+} into the myoplasm and inducing hypercontractive paralysis in skeletal muscle fibers (Fill and Coronado, 1988).

Different striated muscle types express different RyR isoforms, and the mechanism of E-C coupling varies in these tissues. In cardiac muscle, external Ca^{2+} admitted through voltage-gated channels in the plasma membrane triggers Ca^{2+} release from the SR by binding to regulatory sites on RyRs. This mechanism is called "calcium-induced calcium release" (CICR) (Fabiato, 1983). In skeletal muscle, the voltage-gated channels and RyRs appear to be me-

chanically coupled. A conformational change in the plasma membrane channels associated with gating-charge movement directly evokes Ca^{2+} release from RyRs by protein–protein interaction (Rios et al., 1991; Yano et al., 1995). In some vertebrate skeletal muscle more than one RyR isoform (and both E-C coupling mechanisms) are present in the same cells (Airey et al., 1990; Giannini et al., 1995; Jacquemond et al., 1991; O'Brien et al., 1995; Oyamada et al., 1994).

RyRs belong to a family of intracellular Ca^{2+} channels that includes RyRs and inositol trisphosphate receptors (Berridge, 1993). Functional RyR channels are homotetramers composed of subunits of $\sim$565 kD. The channel pore resides in the carboxyl 10–20% of the molecule (Callaway et al., 1994; Meissner et al., 1989), while the bulk of the protein extends into the cytoplasm from the SR membrane (Marty et al., 1994; Radermacher et al., 1994). RyRs have been cloned from a variety of vertebrate and invertebrate species, and are found in a number of tissues in addition to muscle (Giannini et al., 1995; Hakamata et al., 1992; Otsu et al., 1990; Oyamada et al., 1994; Takeshima et al., 1994b, 1989). Sequence analysis of the cloned genes (each about 5,000 amino acids) shows extensive sequence and structural homology, particularly in predicted transmembrane-spanning domains in the carboxyl ends of the proteins (Coronado et al., 1994; McPherson and Campbell, 1993a; Meissner, 1994).

We are investigating the role of RyRs in E-C coupling in *C. elegans* striated muscle. Nematodes have relatively simple body-wall musculature used for locomotion, consisting of rows of longitudinal striated muscle cells on dorsal and ventral sides of the animal (Wood, 1988). Opposing dorsal and ventral muscle cells are coordinately contracted and relaxed, producing sinusoidal waves that propel the animal

---

1. *Abbreviations used in this paper.* E-C coupling, excitation-contraction coupling; RyR, ryanodine receptor; SR, sarcoplasmic reticulum.

forward or backward (Nicholas, 1984). Electrophysiological experiments in *Ascaris lumbricodes* have established that the contractile state of body-wall muscle is controlled by membrane potential (Weisblat et al., 1976; Johnson and Stretton, 1980), which itself is controlled by excitatory and inhibitory inputs from motor neurons (Walrond et al., 1985). Excitatory cholinergic and inhibitory GABAergic neuromuscular synapses have been characterized in *Ascaris* and *C. elegans* (Johnson and Stretton, 1980; Lewis et al., 1987; McIntire et al., 1993), but nothing is known about E-C coupling mechanisms that directly control cytoplasmic Ca^{2+} levels (and therefore contraction) in nematodes. The location and nature of the nematode SR is not certain; it is assumed to consist of vesicular structures that surround dense bodies, the attachment sites for thin filaments in nematode sarcomeres (Nicholas, 1984; Wood, 1988).

C. elegans is known to have RyRs. We characterized a [^{3}H]ryanodine-binding activity in *C. elegans* membranes that copurifies with high conductance ion channels. The channels are cation and Ca^{2+} selective, and are gated by ryanodine (Kim et al., 1992). Addition of ryanodine to the growth medium induces an incomplete hypercontractive paralysis of *C. elegans*, suggesting an effect on body-wall muscle (Kim et al., 1992). Sakube and Kagawal have cloned, sequenced, and characterized a RyR gene in *C. elegans*. This gene, called *ryr-1*, is predicted to encode a protein of 5,017 amino acids that is ~40% identical to cloned RyRs from vertebrates. Ten membrane-spanning domains are predicted in the carboxyl end of *ryr-1*, the region of greatest homology to mammalian RyRs (Sakube et al., 1993). *ryr-1* promoter-β-galactosidase fusion constructs are expressed in adult body-wall muscle and pharyngeal muscle cells (Kagawa, H., personal communication). To better understand the role of RyRs in E-C coupling in nematodes, we undertook a genetic analysis of *ryr-1* in *C. elegans*.

Materials and Methods

Strains and Handling of C. elegans

Handling of *C. elegans* was done using established methods (Wood, 1988). The strains and relevant mutations used were N2 (wild type), MT3126 (*mut-2(r459)*), BC1283 (*sDf30*), MT2583 (*nDf32*), BC1999 (*nDf18*), *unc-68 (e540)*, *unc-70 (e524)*, and *dpy-11 (e224)*. *unc-68* alleles isolated in this study were *r1151::Tc1*, *r1152::Tc1*, *r1158*, *r1160*, *r1161*, *r1162*, *r1167*, *r1207*, *r1208*, *r1209*, *r1210*, *r1211*, *r1212*, *rDf1*, and *rDf2*. The strain TR2267 is homozygous for *r1161*, and contains a stable extrachromosomal array (*rEx95*) containing wild-type *ryr-1* sequences (see below).

Molecular Methods

Preparation of nematode genomic DNA was as previously described (Rushforth et al., 1993). Standard methods were used for preparation of probes, for DNA sequencing, and for hybridization analysis. Screening for Tc1 insertions and deletions was done as described (Rushforth et al., 1993; Zwaal et al., 1993) with some modifications. Populations founded with about 30 MT3126 animals were grown until F2 generation eggs were being laid, and then screened in two-dimensional matrixes. Each population was divided into four parts: two parts were used for the matrix, one part was saved for subdivision, and one part was saved to verify a suspected insertion or deletion. For example, each of 49 populations were assigned a row and a column in a 7 × 7 matrix. Worms from seven populations were pooled for each row or column. DNA prepared from pooled animals in rows and columns was screened with PCR in duplicate. A population having the same polymorphism in both its row and column was further tested by PCR with a third portion of the animals. If positive, the remaining ani-

mals were subdivided into smaller populations and rescreened to ultimately isolate individual animals with insertion or deletion. Single animal PCR was done as described (Williams et al., 1992).

Wild-type *ryr-1* sequences used for transformation rescue were obtained by amplifying three 10.3–10.7-kb fragments from N2 genomic DNA with the Expand™ long template PCR system (Boehringer Mannheim Corp., Indianapolis, IN). The three *ryr-1* primer pair sequence coordinates (5'base and length of primer) are 1,520 (32-mer, sense direction) and 11,870 (32-mer, antisense); 11,440 (39-mer, sense), and 21,770 (35-mer, antisense); 21,361 (25-mer, sense) and 32,145 (35-mer, antisense). The PCR fragments were purified on spin columns, mixed 1:25 with linear DNA fragments (BRL-1-kb ladder), and injected into *unc-68(r1161)* adult hermaphrodites as described (Mello and Fire, 1995) at a total DNA concentration of 100 µg/ml. Transformants were identified by screening the F2 progeny of injected (Unc) animals for animals with wild-type motility.

Isolation of unc-68(r1158)

unc-68 (r1158) was obtained by screening populations of *r1151::Tc1* with flanking primers as described (Zwaal et al., 1993). A 5.4-kb deletion of *ryr-1*, contained in strain TR2125, was identified in this screen. This deletion, *r1158*, removes bps 24,530 to 29,902 of *ryr-1*. TR2125 is phenotypically wild type, but proved to contain a duplication of *ryr-1*. In one copy of *ryr-1*, TR2125 is homozygous for *r1158*. In a second copy, TR2125 is homozygous for *r1151::Tc1*. Both the deletion-containing and insertion-containing alleles of *ryr-1* are tightly linked to *unc-70* (data not shown, see Fig. 1). During these tests of linkage, LGV from TR2125 was placed in trans to *unc-70(e524)*. From one such heterozygote, animals having an Unc phenotype distinct from that of *unc-70* segregated unexpectedly. Southern analysis and PCR tests demonstrated that these novel Unc animals (strain TR2128) were homozygous for *r1158* but no longer contained *r1151::Tc1*. We have not characterized further the duplication/deletion rearrangement of TR2125, but we presume that the simple deletion *r1158* in TR2128 represents resolution of the duplication via homologous recombination.

Noncomplementation Screens

In the screen for new spontaneous alleles, wild-type males were crossed to *r1151::Tc1* or *r1152::Tc1* hermaphrodites. The resulting *ryr-1::Tc1/+* males were then crossed to *dpy-11(e22) unc-68(r1158)* homozygotes. The F1 progeny were then screened for Unc non-Dpy hermaphrodites. Putative new *unc-68* alleles were outcrossed, tested for complementation with *unc-68(e540)*, and checked for the absence of the *r1158* deletion with PCR. New alleles were characterized with PCR and Southern analysis. In the screen for EMS-induced alleles, wild-type males were mutagenized with EMS (Anderson, 1995) and crossed with *dpy-11(e224) unc-68(r1158)* hermaphrodites as above. Putative new EMS-induced alleles were outcrossed, tested for complementation with *unc-68(e540)*, and checked for the absence of the *r1158* deletion with PCR. Six new alleles were designated *r1207–r1212*.

Binding Assays and Membrane Purification

Whole *C. elegans* were collected, floated on 35% sucrose (Wood, 1988) and washed in H_2O. Washed worms were resuspended in 20 mM MOPS, pH 7.2, in a protease inhibitor cocktail previously described (Kim et al., 1992). Worms were homogenized by passing twice through a french pressure cell at 10,000 psi. To purify the microsomal fraction, the crude homogenates were spun at 2,400 *g* for 30 min in corex tubes. The supernatant was layered on an equal volume of 30% sucrose (in 0.4 m KCl, 20 mM MOPS, pH 7.2, pCa 4.3) and spun at 90,000 *g* for 45 min. The pellets were resuspended in 1.0 M KCl, 20 mM Tris, pH 8.0, pCa 4.3. Binding assays were done in resuspension buffer at 37°C with indicated concentrations of [^{3}H]ryanodine (Dupont-New England Nuclear, Boston, MA). Assays were in triplicate, with 70 µg microsomal protein per sample. Bound [^{3}H]ryanodine was collected on glass fiber filters and counted in scintillation cocktail as described (Kim et al., 1992). Specific counts for each ryanodine concentration were determined by subtracting counts bound in the presence of 100 µM unlabeled ryanodine (Agrisystems International, Wind Gap PA) from counts in the presence of labeled ryanodine only.

Electron Microscopy

Animals were fixed for 1 h on ice in a solution composed of 0.67% fresh glutaraldehyde and 0.67% osmium tetroxide in 0.1 M cacodylate buffer,

pH 7.4 (C buffer). The heads were cut off, the animals washed three times in C buffer, and then incubated at 4°C overnight in 2% osmium tetroxide in C buffer. Animals were washed again, dehydrated, and embedded in Spurr's resin. Adult hermaphrodites were sectioned perpendicular to the long axis of the body posterior to the terminal bulb of the pharynx. The sections were viewed in a JEOL (Peabody, MA) 100 electron microscope at a magnification 19,000.

Results

Genetic and Physical Location of ryr-1

A *C. elegans* ryanodine receptor homologue cDNA (cm16C2) was identified in a screen of expressed genes (Waterston et al., 1992). The sequence of cm16C2, a 1,232-bp partial cDNA of *ryr-1*, is homologous over its entire length to several mammalian ryanodine receptors in the databases (~30% identical). cm16C2 hybridized to three overlapping YACs on linkage group V (see Fig. 1). These YACs span the interval between *snb-1* and *odr-2*, two genes whose positions are known on both the physical and genetic maps (see Fig. 1). We located cm16C2 more precisely on the genetic map using several overlapping deficiencies affecting this region. Deficiency homozygote embryos were tested with PCR for cm16C2 sequences. cm16C2 (*ryr-1*) mapped to an interval of ~0.1 map units bounded
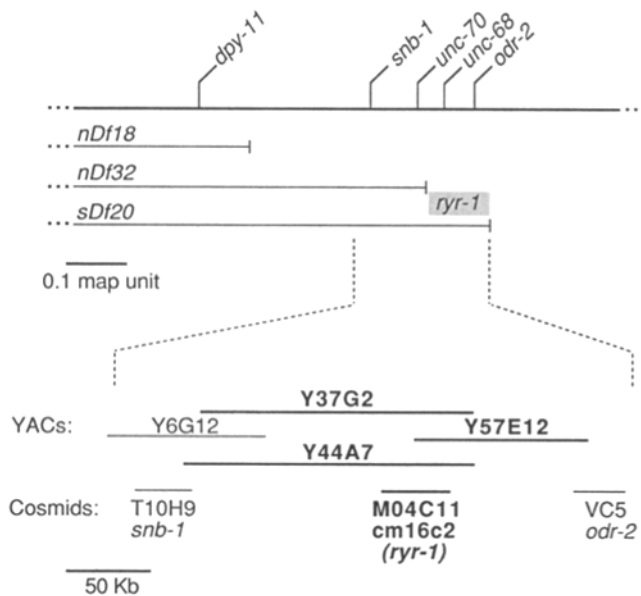
Figure 1. Physical and genetic maps of LGV surrounding *ryr-1*. The partial *ryr-1* cDNA cm16c2 hybridized to three (*bold type*) of four overlapping YACs shown in the expanded area. *ryr-1* is ordered on the YAC contig with respect to *snb-1* and *odr-2*, two genes whose location is known on both genetic and physical maps. Cosmids having all or a portion of *snb-1*, *odr-2*, or *ryr-1* are shown with gene names below the contig. *snb-1* and *odr-2* are also ordered on the genetic map above with respect to *dpy-11*, *unc-70*, *unc-68*, and three deficiencies: *nDf18*, *nDf32*, and *sDf30*. The shaded area shows the interval to which the cm16C2 clone mapped. The relative order of *snb-1* and *unc-70* has recently been established (Nonet, M., and E. Jorgensen, personal communication).

by the right breakpoints of deficiencies *nDf32* and *sDf20* (see Fig. 1, *shaded area*). This interval contains *unc-68* and *odr-2*, and eight complementation groups defined by recessive lethal mutations (Johnson and Baillie, 1991).
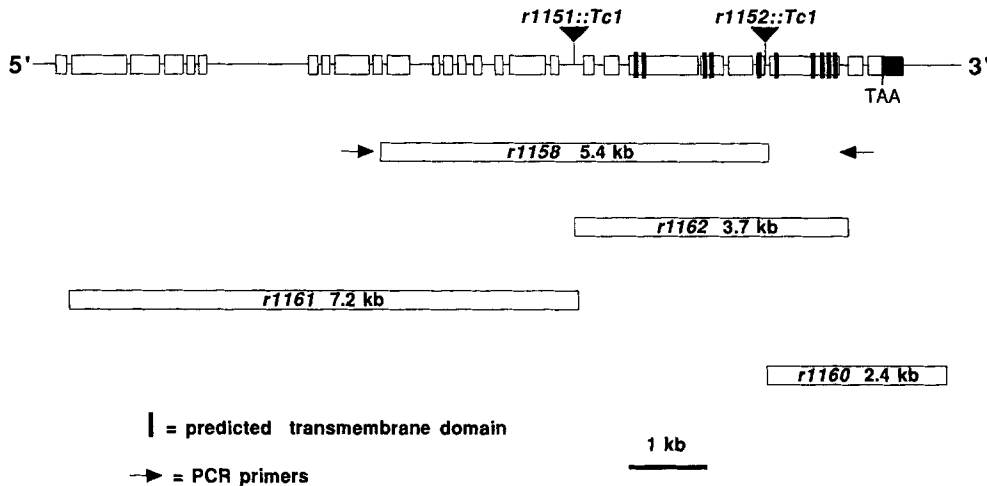
Site-selected Tc1 Insertions within ryr-1

Y. Sakube and H. Kagawa independently identified *ryr-1*, and determined the complete sequence of both genomic and cDNA clones. ryr-1 is composed of 46 exons spanning over 30-kb of genomic DNA (see Fig. 2). With genomic sequence information generously provided by Sakube and Kagawa, we screened for animals having Tc1 transposable element insertions within the 3' third of *ryr-1*. Using a PCR/sib-selection method previously described (Rushforth et al., 1993), two site-selected Tc1 insertions were obtained (see Fig. 2). Sequencing of PCR fragments spanning the insertion junctions revealed that *r1151* contained an insertion within intron 37 at TA dinucleotide 27,147–27,148 (coordinates of Sakube et al., Genbank accession number D54899) and *r1152* contained an insertion within the 5' splice donor of intron 43 (TA dinucleotide 29,618–29,619). Southern hybridization of DNA from insertion homozygotes confirmed the size and location of the Tc1 insertions in *r1151* and *r1152* (Fig. 3, lanes 2 and 9, respectively). Both *r1151* and *r1152* homozygotes are wild-type in phenotype.

Isolation of ryr-1 Deletions

Because Tc1 sequences are spliced from most, if not all Tc1-containing pre-mRNAs (Rushforth and Anderson, 1996), we suspected that the wild-type phenotypes of *r1151* and *r1152* did not represent the *ryr-1* null phenotype. Using previously described methods (Zwaal et al., 1993), we isolated *r1158*, an excision derivative of *r1151::Tc1*, in which 5.4 kb of *ryr-1* are deleted (see Fig. 2 and 3, lane 3). Sequencing of the *r1158* deletion junction (generated by PCR) demonstrated that *ryr-1* coordinates 24,531 to 29,901 (inclusive) are deleted in *r1158*. *r1158* homozygotes are uncoordinated and exhibit a phenotype that is identical to that of *unc-68(e540)*, the *unc-68* reference allele. Furthermore, *r1158* fails to complement *unc-68(e540)*.

To confirm that the Unc-68 phenotype of *r1158* was caused by the *ryr-1* deletion, a noncomplementation screen for new alleles of *unc-68* was performed, using *r1151::Tc1* and *r1152::Tc1* as a source of new mutations. Our expectation was that imprecise excision of Tc1 in a mutator background would yield additional deletion alleles of *ryr-1* at relatively high frequency (Zwaal et al., 1993). If the Unc-68 phenotype of *r1158* were due to a mutation in a gene other than *ryr-1*, then the frequency of new *unc-68* alleles would be very low, or the deletions obtained from Tc1 excisions would always extend beyond *ryr-1* and include nearby genes. Six new spontaneous alleles of *unc-68* were isolated from 2,330 *r1151::Tc1* and *r1152::Tc1* chromosomes screened (see Materials and Methods). Three of these alleles (*r1160*, *r1161*, and *r1162*) delete the Tc1 element used to generate them as well as 2.4–7.2 kb of adjacent *ryr-1* sequences (see Fig. 2, also see Fig. 3, lanes 4, 6, and 9). Two alleles (*rDf1* and *rDf2*) contain deletions that, based on PCR tests, extend beyond *ryr-1* coding sequences. Both *rDf1* and *rDf2* are lethal as homozygotes,

ryr-1 Genomic Region: Exons 20-46

Figure 2. Tc1 site-selected insertions and Tc1-induced deletions. Exons 20-46 of *ryr-1* showing the location of two Tc1 insertions and four deletions. *r1158* was isolated from *r1151::Tc1* using the primer pair shown (see Materials and Methods). Three alleles isolated in a noncomplementation screen (*r1160, r1161, r1162,* see Materials and Methods) are deletions within *ryr-1* that extended unidirectionally from the Tc1 insertion from which they were derived. *r1161* and *r1162* were derived from *r1151,* while *r1160* was derived from *r1152.* The sizes of *r1158, r1160,* and *r1162* were determined by sequencing deletion junction fragments. The size of *r1161* was estimated from Southern analysis and from the size of PCR fragments amplified from primers flanking the deletion. Ten predicted transmembrane-spanning domains are shown as vertical black bars (Sakube et al., 1993).

presumably because they delete other genes in addition to *ryr-1.* A sixth allele (*r1167,* see Fig. 3, lane *10*) retains the *r1152::Tc1* insertion. It is being further characterized to determine the nature of its new mutation.

Rescue of unc-68 with ryr-1 Genomic DNA

As further proof that *unc-68* and *ryr-1* are synonymous, *ryr-1* genomic DNA was used for transformation rescue of *unc-68* mutants (Mello and Fire, 1995). The cosmid M04C11 (see Fig. 1) contains the entire *ryr-1* coding sequence, but M04C11 DNA failed to rescue the Unc-68 phenotype. Y. Sakube and H. Kagawa have shown that body-wall muscle expression of *ryr-1* requires noncoding upstream regulatory sequences not present in M04C11 (Kagawa, H., personal communication). We therefore used PCR to amplify *ryr-1* and 3 kb of upstream sequence from N2 genomic DNA in three 10.3–10.7-kb fragments, which together span *ryr-1* sequence coordinates 1,520–32,145 (see Materials and Methods). The central fragment overlapped the 5' and 3' fragments by 300–350 bp to allow homologous recombination in vivo (see Mello and Fire, 1995).

The three PCR fragments were injected into *unc-68(r1161)* hermaphrodites. F2 progeny of the injected Unc animals included wild-type hermaphrodites. One such animal established the strain TR2267, which carries an extrachromosomal array (*rEx95*) that includes *unc-68*(+). TR2267 wild-type hermaphrodites segregate wild-type and Unc progeny. PCR of TR2267 wild-type animals showed that both the *r1161* deletion and wild-type alleles of *ryr-1* were present, while TR2267 Unc animals contained only the *r1161* deletion allele. *rEx95* was also able to rescue other *unc-68* alleles, including *e540,* as shown by crossing wild-type TR2267 males to *unc-68* homozygotes and recovering wild-type F1 progeny. These experiments demonstrate

that *unc-68* and *ryr-1* are the same gene. Hereafter, we refer to this gene simply as *unc-68.*

unc-68 Null Phenotype

Three lines of evidence indicate that the viable, uncoordinated phenotype of the *unc-68* deletion homozygotes represents the *unc-68* null phenotype. First, the four deletions remove substantial (and differing) portions of the *unc-68* coding sequence, yet exhibit the same Unc-68 phenotypes. In particular, *r1162* deletes all of the predicted membrane-spanning domains (Sakube et al., 1993) (see Fig. 2). Since homologous domains in mammalian RyRs appear to contain the channel pore (Callaway et al., 1994, Meissner et al., 1989) *r1162* is certainly a "channel null" allele, regardless of whether it is a protein null allele. Second, the deletion mutations are fully recessive, and their Unc-68 phenotype is not more severe when any of them is placed in *trans* to a large deficiency that removes all of *unc-68* (*sDf20,* see Fig. 1). Third, new alleles of *unc-68* that are indistinguishable from those described above arise at high frequency following EMS mutagenesis. From 2871 EMS-mutagenized chromosomes, we isolated six new *unc-68* alleles (see Materials and Methods). Such frequencies of isolation suggest that the Unc-68 phenotype is due to loss of function alleles (Anderson, 1995).

Effects of unc-68 Mutations on Muscle Function

Wild-type *C. elegans* moves by propagating sinusoidal contraction waves in strips of striated muscle cells attached to the cuticle along the body length (Croll, 1975; Nicholas, 1984). Contraction waves of *unc-68* homozygotes propagate more slowly than those of wild type. *unc-68* mutants move slowly, and exhibit a languid, incomplete flaccid paralysis. The animals travel for shorter average distances
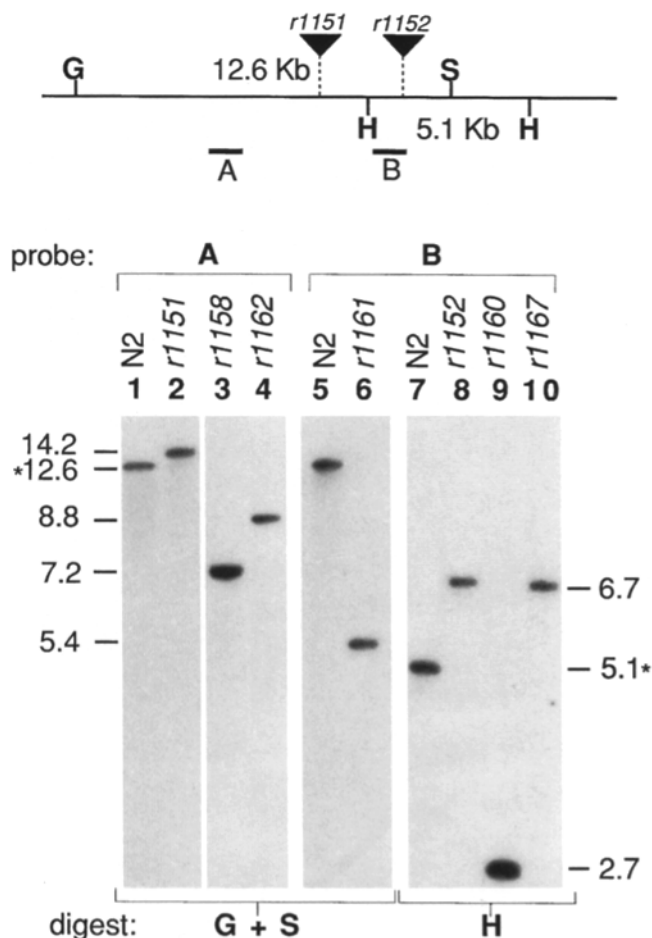
Figure 3. Southern hybridization analysis of Tc1 insertion and deletion mutants. Genomic DNA from wild-type or *unc-68* mutants was digested with BglII (*G*) + SpeI (*S*), or HindIII (*H*). Filter strips from the same gel were hybridized to probe *A* or *B*, as indicated above the lanes. The sizes of the hybridizing bands are shown in kilobases at left for BglII + SpeI digests, or at right for HindIII digests. Restriction sites and fragment sizes of N2 DNA (wild type), and the location of probes *A* and *B* are shown on the map above. Also indicated are the locations of the Tc1 insertions. The map shows *ryr-1* (*unc-68*) sequences from the BglII site at bp 19,263, (exon 19) to the HindIII site at bp 34,321, 2.2 kb 3' of the poly-A addition site (Sakube et al., 1993).

than wild type, are immobile for more extended periods of time, and assume unusual extended or curled body postures. In a motility assay performed in liquid media, *unc-68* mutants propagated 25–30% the number of contraction waves observed in wild-type animals (see Table I). As shown in Table I, the motility of *unc-68(r1161)* was restored to wild-type level by rescue with the *unc-68(+)* array (see *r1161;rEx95*).

unc-68 mutants do not exhibit defects of anal depressor or sex muscles, although pharyngeal muscle function may be affected. Defecation is grossly normal (Reiner, D., and J. Thomas, personal communication), and *unc-68* mutants are proficient in egg laying. While *unc-68* males mate poorly, this is most likely a consequence of their impaired motility. Pharyngeal pumping is somewhat weaker in *unc-68* mutants than in wild-type, although electrical activity during pharyngeal muscle contraction is normal in *unc-68* mutants (Lee, R., and L. Avery, personal communication). The mutants grow more slowly than their wild-type counterparts, perhaps due to weaker pumping (feeding) during larval development.

Body-Wall Muscle Ultrastructure Is Normal in unc-68 Mutants

The motility defects of *unc-68* mutants could arise from structural abnormalities of the muscle contractile apparatus, or from defective regulation of contraction. We compared wild-type and *unc-68* body-wall muscle using electron microscopy. *unc-68* sarcomeres exhibit nearly wild-type ultrastructure, as seen in transverse sections (see Fig. 4). The distribution of thick and thin filaments, and the number and location of dense bodies and M-lines (Wood, 1988) were essentially normal in *unc-68* animals. We observe two subtle irregularities in *unc-68* body-wall muscles. First, the depth of the spindle region (but not its myofilament organization) is more heterogeneous. Thus, many *unc-68* sarcomeres are deeper than their wild-type counterparts. Second, dense bodies are more often irregular in shape than wild type (e.g., lower left image in Fig. 4). We conclude from this analysis that *unc-68* body-wall muscle ultrastructure is nearly normal, and that motility defects are due to defective regulation of contraction.

unc-68 Mutants Are Insensitive to Ryanodine

Contraction of body-wall muscle is impaired, but not eliminated in *unc-68* mutants. Because many species express

*Table I. Motility Assay for Wild-type and unc-68 Mutant Animals*

		unc-68 allele						
		W.T.	e540	r1158	r1160	r1162	r1161	r1161; rEx95
− Ryanodine	exp. 1	107 ± 8	29 ± 4.6	29 ± 5.5	27 ±4.4	22 ± 4.0	25 ± 4.5	103 ± 8.1
	exp. 2	114 ± 18	28 ± 3.8	28 ± 5.0	27 ± 4.1	22 ± 5.0	24 ± 4.4	104 ± 8.6
+ Ryanodine	exp. 1	12 ± 1.9	30 ± 4.6	29 ± 5.5	28 ± 7.5	23 ± 4.9	25 ± 4.7	8 ± 1.6
	exp. 2	12 ± 2.6	28 ± 6.3	28 ± 3.5	27 ± 5.3	23 ± 5.3	23 ± 3.7	9 ± 1.6

The relative motility of wild-type and *unc-68* mutants was measured by counting the waveforms (Croll, 1975) propagated by individual animals in one minute. Each value is the average number of waveforms counted (± SD) in ten animals. Before counting, adult hermaphrodites were placed in 24-well plates in 0.5 ml S-media (Wood, 1988) with or without 2 μM ryanodine. The plates were incubated at room temperature, while shaking, until wild-type animals were fully contracted by ryanodine (at least 30 min). A waveform was defined as the propagation of a contraction wave from head-to-tail, from tail-to-head, or the curling and uncurling of the body. Results from two independent experiments are shown.
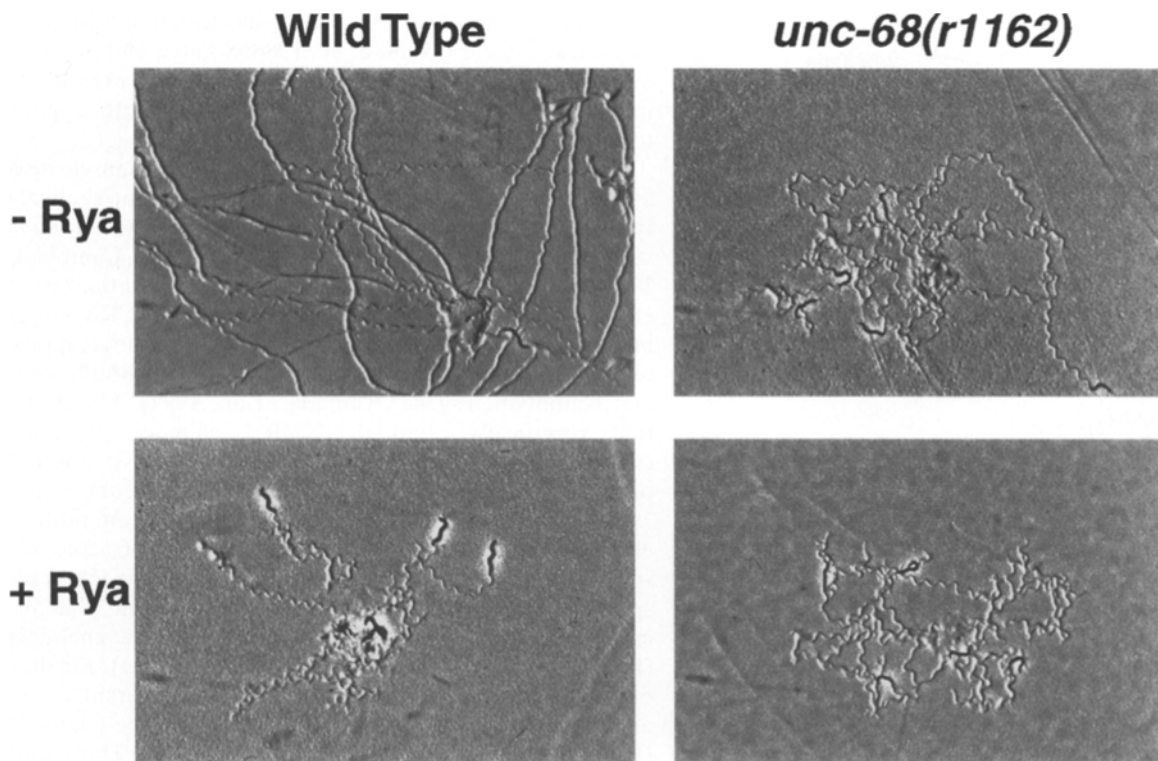
Wild Type
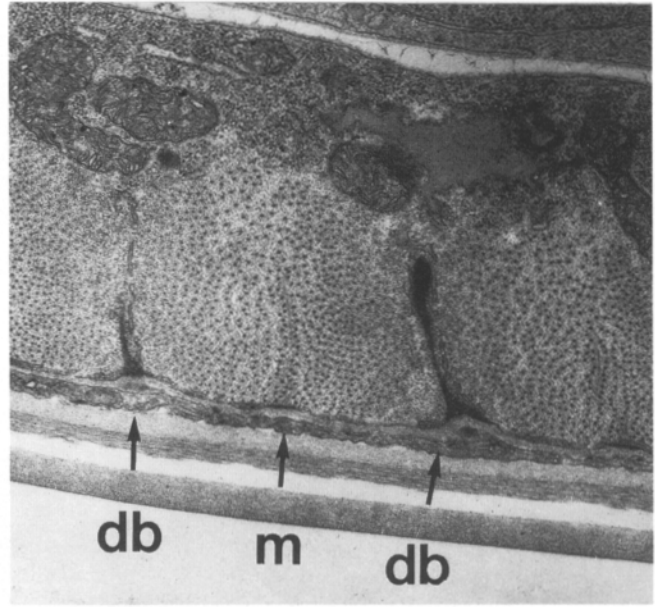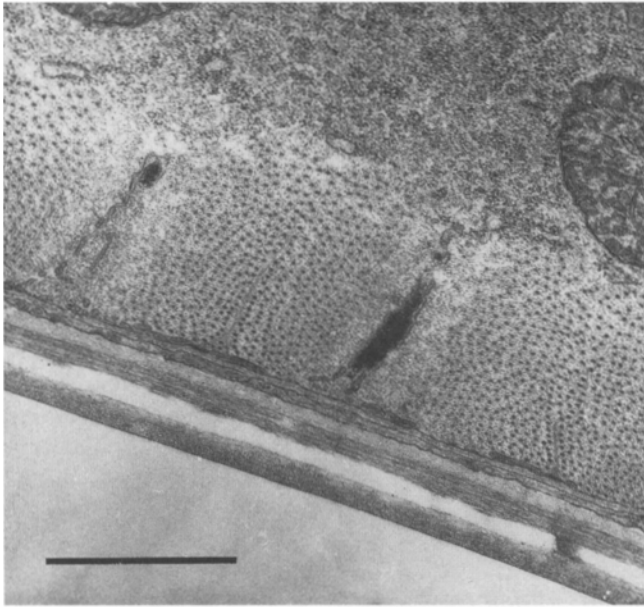
unc-68(r1162)
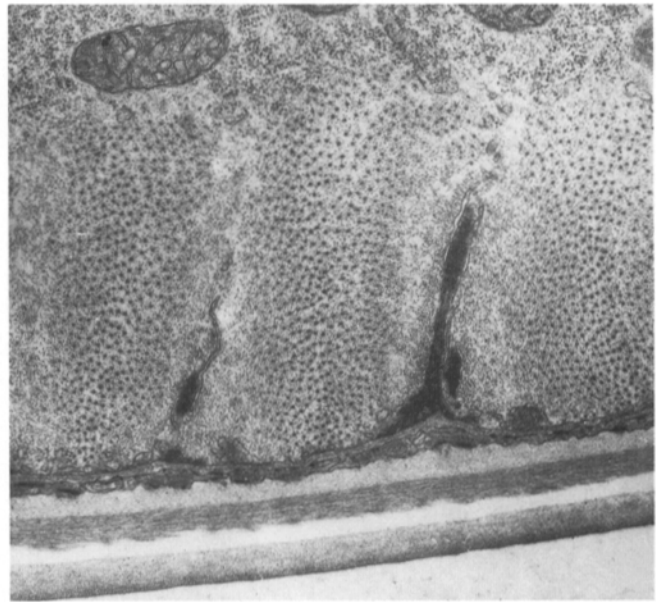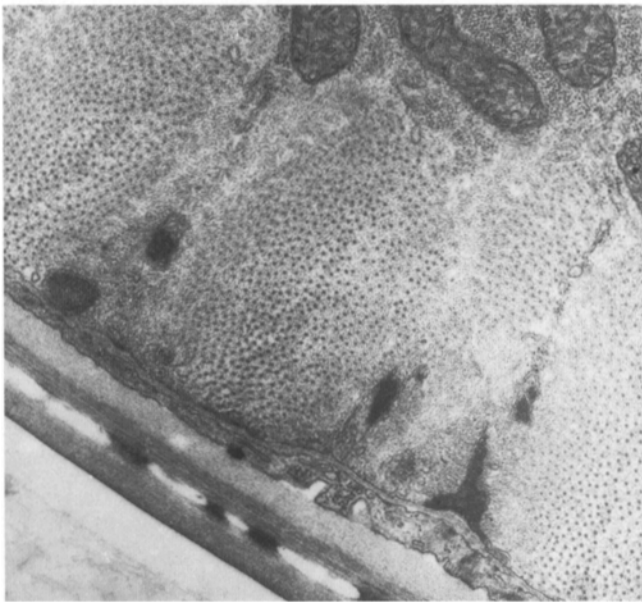
Figure 4. Transverse sections of wild-type (N2) and *unc-68* body-wall muscle. Wild type or *unc-68* (*r1162*) animals were prepared for EM as described in Materials and Methods. Transverse sections from adult hermaphrodites taken posterior to the terminal bulb of the pharynx are shown. Magnification, 19,000. *db*, dense bodies; *m*, M line (Nicholas, 1984; Wood, 1988) *unc-68* (*r1162*) exhibits nearly normal muscle ultrastructure. Bar, 1.0 μM.

two RyR isoforms in the same muscle cell type (Airey et al., 1990; Giannini et al., 1995; O'Brien et al., 1993; Oyamada et al., 1994), we tested *unc-68* mutants for sensitivity to contraction by ryanodine, which induces incomplete hypercontractive paralysis of *C. elegans* (Kim et al., 1992). After exposure to ryanodine, wild-type animals become shorter and thicker, indicating that the body-wall muscles are hypercontracted. Wild-type animals in 2 mM ryanodine move very slowly compared to animals without drug, as shown in a motility assay (see Table I), and by the length of tracks left in bacterial lawns (Fig. 5). In contrast, *unc-68* mutants are completely resistant to ryanodine.

Wild Type **unc-68(r1162)**

- Rya

+ Rya

Figure 5. Effect of ryanodine on the motility of wild-type or *unc-68* animals. Five adult hermaphrodites were placed on 35-mm agar plates having bacterial lawns. Ryanodine-treated animals were first incubated in M9 media (Wood, 1988) containing 2 μM ryanodine for 30 min (a time sufficient to maximally paralyze wild type), and then placed on agar plates containing 2 μM ryanodine. After 10 min, the plates were photographed through a Wild M3Z dissecting microscope equipped with a phototube. In the picture showing wild-type without ryanodine *(top left)*, the animals made extensive tracks covering the plate, only some of which are visible in the field.

Both the *unc-68* deletion mutants described above and the *unc-68* reference allele *e540* are unaffected by 2 mM ryanodine, a concentration 20 times higher than the minimum required to paralyze wild type (see Table I and Fig. 5). Rescue of *unc-68(r1161)* with the wild-type *unc-68* gene restored sensitivity to ryanodine (see *r1161; rEx95*, Table I). These experiments show that *unc-68*–encoded RyRs alone are responsible for the effects of ryanodine on body-wall muscle function.

unc-68 Mutants Lack Ryanodine-binding Activity

Microsomes prepared from *C. elegans* homogenates contain a saturable, high affinity [³H]ryanodine-binding activity. Although the amount of binding activity is low in comparison to rabbit skeletal muscle, the binding affinity (K_d 26 nM) is similar to that measured for vertebrate RyRs (Kim et al., 1992). If *unc-68* encodes the only RyR in *C. elegans* (as defined by ryanodine binding), then *unc-68* mutants should lack high affinity ryanodine-binding activity. We measured [³H]ryanodine binding in microsomes prepared in parallel from wild-type or *unc-68* mutants. One such experiment is shown in Fig. 6. We were unable to detect specific [³H]ryanodine binding in *unc-68* microsomes, while those from wild-type animals contained saturable, high affinity [³H]ryanodine-binding sites. These data, together with the ryanodine resistance of *unc-68* mutants, suggest that *unc-68* encodes the only RyR in *C. elegans*.

Discussion

We provide five lines of evidence demonstrating that *unc-68* encodes a ryanodine receptor (RyR) involved in regulating *C. elegans* body-wall muscle contraction. First, the cloned RyR gene *ryr-1* (Sakube et al., 1993) maps to a genetic interval that includes *unc-68*, and intragenic deletions of *ryr-1* isolated with reverse genetic methods and noncomplementation screens are alleles of *unc-68*. Second, transformation of *unc-68* mutants with *ryr-1* sequences fully rescues the Unc-68 phenotype. Third, *unc-68* mutants exhibit motility defects (incomplete paralysis), but their body-wall muscle ultrastructure is essentially normal. Fourth, *unc-68* mutants are insensitive to the paralyzing effects of ryanodine. Fifth, microsomal fractions of *unc-68* mutants are devoid of the high affinity binding activity that characterizes wild-type microsomes.

Sakube and Kagawa have shown that *unc-68* is expressed in body-wall muscle cells (Kagawa, H., personal communication). *ryr-1* promoter fusions to *lacZ* are expressed in body-wall muscle cells, and are variably expressed in pharyngeal muscle and in egg-laying muscles. We and others have not observed severe behavioral defects of *unc-68* mutants in pharyngeal pumping or egg laying, although the weaker pumping (Lee, R., and L. Avery, personal communication) and slow larval growth (Maryon, E., unpublished results) of *unc-68* mutants suggest a role of *unc-68* in the regulation of pharyngeal muscle contraction.
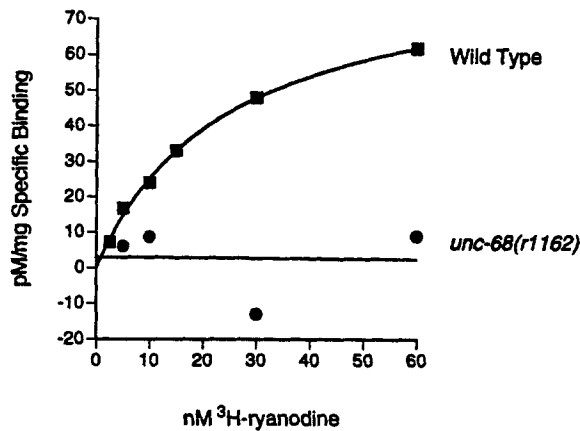
Figure 6. [³H]Ryanodine binding to *C. elegans* microsomes. Microsomes were prepared from either wild-type or *unc-68 (r1162)* mutants as described in Materials and Methods. After incubation for 2 h at 37°C in [³H]ryanodine at indicated concentrations, the bound counts were collected on glass fiber filters. Samples were assayed in triplicate for specific and nonspecific binding. Specific binding was calculated as average [³H]ryanodine counts bound at a given drug concentration in excess of the counts bound in the presence of 100 μM unlabeled ryanodine. The calculated K_d of [³H]ryanodine binding to wild-type microsomes was 24 nM, close to the value of 26 nM obtained in earlier studies (Kim et al., 1992).

RyRs play an important, but nonessential role in E-C coupling in *C. elegans* body-wall muscle. *unc-68* appears to encode the only RyR expressed in *C. elegans*, since *unc-68* mutants are resistant to the paralytic effects of ryanodine and lack detectable [³H]ryanodine-binding activity. Based on these observations, RyRs are not necessary for contraction of body-wall muscle because *unc-68* mutants propagate attenuated sinusoidal contraction waves up or down the body length (see Table I and Fig. 5). Furthermore, in wild-type animals, ryanodine induces an incomplete paralysis. At high drug concentration, the hypercontracted animals still move with slow, sinusoidal motion, as shown by the tracks left in bacterial lawns (see Fig. 5). Thus, coordinated contraction and relaxation of body-wall muscle cells still occurs with either a (presumed) deficit of RyR-supplied Ca^{2+} in *unc-68* mutants or an excess of Ca^{2+} in the presence of ryanodine. Wild-type RyR function greatly enhances motility (see Table I and Fig. 5), but is not necessary for E-C coupling per se.

The RyR-independent contraction observed in *unc-68* body-wall muscle cells could be initiated by Ca^{2+} from an external or internal source. In many invertebrates, including nematodes, muscle plasma membrane depolarization emanates from neuromuscular junctions as a graded Ca^{2+} spike (Hagiwara and Naka, 1964; Weisblat et al., 1976). In *C. elegans*, Ca^{2+} entering through plasma membrane voltage-gated channels might suffice to initiate contraction, unlike the modest Ca^{2+} flux through analogous channels in cardiac myocytes (Varro et al., 1993). The small size of body-wall muscle cells and close proximity of sarcomeres to the plasma membrane could reduce the need for internal Ca^{2+} release. On the other hand, an internal Ca^{2+} source cannot be ruled out. For example, cardiac myocytes

and smooth muscle cells contain inositol trisphosphate-gated Ca^{2+} stores (Otani et al., 1988; Somlyo and Somlyo, 1994). Regardless of the source of Ca^{2+} that evokes RyR-independent contraction in *unc-68* mutants, RyRs appear to amplify the signal in body-wall muscle cells.

Certain RyR isoforms in vertebrate skeletal muscle also appear to amplify calcium transients. The major skeletal-type RyRs, termed RYR-1 in mammals or α-RyR in other vertebrates (Airey et al., 1990; McPherson and Campbell, 1993a), are directly gated by membrane potential (Rios et al., 1991). A second skeletal isoform, termed RYR-3 in mammals or β-RyR in other vertebrates, does not respond directly to depolarization (Airey et al., 1990, McPherson and Campbell, 1993a; Oyamada et al., 1994). Mutations that specifically eliminate RYR-1 channels in mice (*skrr^{m1}*) or α-RyRs in chickens (cn) have recessive lethal phenotypes, resulting in perinatal death (Ivanenko et al., 1995; Takeshima et al., 1994a). Muscle fibers from mutant embryos lack normal Ca^{2+} transients or contractile responses upon electrical stimulation, but exhibit these responses when exposed to caffeine or treatments that increase Ca^{2+} entry through plasma membrane channels (Ivanenko et al., 1995; Takeshima et al., 1994a). Further experiments suggest that the responses of mutant fibers are due to CICR through RyR-3 or β-RyR-type channels (Percival et al., 1994; Takeshima et al., 1995). These and other experiments have provoked a two receptor model for Ca^{2+} release in skeletal muscle, in which β-type RyRs amplify the Ca^{2+} released by α-type RyRs by CICR (Ivanenko et al., 1995; Jacquemond et al., 1991; O'Brien et al., 1995).

The amplification of Ca^{2+} signals by CICR is probably the more ancient and most common role of RyRs in E-C coupling. The major skeletal isoforms (and "mechanical" E-C coupling) appear to have evolved from β-RyR-type channels to serve the needs of fast twitch muscle types (O'Brien et al., 1993). Other RyR isoforms in cardiac muscle, in smooth muscle, in crustaceans, and in the CNS are known (or believed) to use a CICR mechanism (Fabiato, 1983; Györke and Palade, 1992; Lynn and Gillespie, 1995; McPherson and Campbell, 1993b). We infer from the Unc-68 phenotype that RyRs in nematodes, one of the more primitive metazoan phyla, also amplify Ca^{2+} signals. While there is no direct evidence of a CICR mechanism for nematode RyRs, it is notable that UNC-68 is more similar to cardiac RyRs than to the major skeletal isoforms (Sakube et al., 1993).

Our experiments lead us to conclude that the role of RyRs in *C. elegans* body-wall muscle is to enhance contraction by amplifying a depolarization-coupled Ca^{2+} transient. We consider it less likely that RyRs are involved in relaxation (e.g., repolarization of the muscle membrane), as proposed for RyRs in arterial smooth muscle cells (Nelson et al., 1995), because the absence of RyR function in *unc-68* mutants results in languid, flaccid paralysis, while ryanodine, known to lock the channels open, causes hypercontraction of wild-type animals. Further studies of *unc-68*-encoded RyR channels will help to uncover the molecular mechanisms regulating nematode body-wall muscle contraction, and should also be useful in understanding the evolution of RyRs and E-C coupling in more complex organisms.

References

Airey, J.A., C.F. Beck, K. Murakami, S.J. Tanksley, T.J. Deerinck, H. Ellisman, and J.L. Sutko. 1990. Identification and localization of two triad junctional foot protein isoforms in mature avian fast twitch skeletal muscle. *J. Biol. Chem.* 265:14187–14194.

Anderson, P. 1995. Mutagenesis. *In* Methods in Cell Biology. Vol. 48. H.E. Epstein and D.C. Shakes, editors. Academic Press, San Diego. 31–54.

Berridge, M.J. 1993. Inositol triphosphate and calcium signalling. *Nature (Lond.).* 361:315–325.

Callaway, C., A. Seryshev, J.P. Wang, K.J. Slavik, D.H. Needleman, C. Cantu, Y. Wu, T. Jayaraman, A.R. Marks, and S.L. Hamilton. 1994. Localization of the high and low affinity [³H]ryanodine binding sites on the skeletal muscle Ca⁺ release channel. *J. Biol. Chem.* 280:15876–15884.

Caterall, W.A. 1991. Excitation-contraction coupling in vertebrate skeletal muscle: a tale of two calcium channels. *Cell.* 64:871–874.

Coronado, R., J. Morrissette, M. Sukhareva, and D.M. Vaughan. 1994. Structure and function of ryanodine receptors. *Am. J. Physiol.* 94:1485–1504.

Croll, N.A. 1975. Components and patterns in the behavior of the nematode *Caenorhabditis elegans. J. Zool. Lond.* 176:159–176.

Fabiato, A. 1983. Calcium-induced release of calcium from the cardiac sarcoplasmic reticulum. *Am. J. Physiol.* 245:C1–C14.

Fill, M., and R. Coronado. 1988. Ryanodine receptor channel of sarcoplasmic reticulum. *Trends Neurosci.* 11:453–457.

Giannini, G., A. Conti, S. Mammarella, M. Scrobogna, and V. Sorrentino. 1995. The ryanodine receptor/calcium channel genes are widely and differentially expressed in murine brain and peripheral tissues. *J. Cell Biol.* 128:893–904.

Györke, S., and P. Palade. 1992. Calcium-induced calcium release in crayfish skeletal muscle. *J. Physiol.* 457:195–210.

Hagiwara, S., and K.-I. Naka. 1964. The initiation of spike potential in barnacle muscle fibers under low intracellular Ca⁺⁺. *J. Gen. Physiol.* 48:141–162.

Hakamata, Y., J. Nakai, H. Takeshima, and K. Imoto. 1992. Primary structure and distribution of a novel ryanodine receptor/calcium release channel from rabbit brain. *FEBS Lett.* 312:229–235.

Ivanenko, A., D.D. McKemy, J.L. Kenyon, J.A. Airey, and J.L. Sutko. 1995. Embryonic chicken skeletal muscle cells fail to develop normal excitation-contraction coupling in the absence of the α-ryanodine receptor. *J. Biol. Chem.* 270:4220–4223.

Jacquemond, V., L. Csernoch, M.G. Klein, and M.F. Schneider. 1991. Voltage-gated and calcium-gated calcium release during depolarization of skeletal muscle fibers. *Biophys. J.* 60:867–873.

Johnson, C.D., and A.O.W. Stretton. 1980. Neural control of locomotion in *Ascaris*: anatomy, physiology, and biochemistry. *In* Nematodes as Biological Models. Vol. 1. B.M. Zuckerman, editor. Academic Press, New York. 159–195.

Johnson, R.C., and D.L. Baillie. 1991. Genetic analysis of a major segment [LGV(left)] of the genome of *Caenorhabditis elegans. Genetics.* 129:735–752.

Kim, Y.K., H.H. Valdivia, E.B. Maryon, P.A. Anderson, and R. Coronado. 1992. High molecular weight proteins in the nematode *C. elegans* bind [³H] ryanodine and form a large conductance channel. *Biophys. J.* 63:1379–1384.

Lewis, J.A., J.S. Elmer, J. Skimming, S. Mclafferty, J. Flemming, and T. McGee. 1987. Cholinergic receptor mutants of the nematode *Caenorhabditis elegans. J. Neurosci.* 7:3059–3071.

Lynn, S., and J.I. Gillespie. 1995. Basic properties of a novel ryanodine-sensitive, caffeine-insensitive calcium-induced calcium release mechanism in permeabilized human vascular smooth muscle cells. *FEBS Lett.* 367:23–27.

Marty, I., M. Villaz, G. Arlaud, I. Bally, and M. Ronjat. 1994. Transmembrane orientation of the N-terminal and C-terminal ends of the ryanodine receptor in the sarcoplasmic reticulum of the rabbit skeletal muscle. *Biophys. J.* 298: 743–749.

McIntire, S.L., E. Jorgensen, and H.R. Horvitz. 1993. Genes required for GABA function in *Caenorhabditis elegans. Nature (Lond.).* 364:334–337.

McPherson, P.S., and K.P. Campbell. 1993a. The ryanodine receptor/Ca²⁺ release channel. *J. Biol. Chem.* 268:13765–13768.

McPherson, P.S., and K.P. Campbell. 1993b. Characterization of the major brain form of the ryanodine receptor/Ca²⁺ release channel. *J. Biol. Chem.* 268:19785–19790.

Meissner, G. 1994. Ryanodine receptor/Ca²⁺ release channels and their regulation by endogenous effectors. *Annu. Rev. Physiol.* 56:485–508.

Meissner, G., E. Rousseau, and F.A. Lai. 1989. Structural and functional correlation of the trypsin-digested Ca²⁺ release channel of skeletal muscle sarco-

plasmic reticulum. *J. Biol. Chem.* 264:1715–1722.

Mello, C., and Fire, A. 1995. DNA transformation. *In* Methods in Cell Biology. Vol. 48. H.E. Epstein and D.C. Shakes, editors. Academic Press, San Diego, CA. pp. 452–482.

Nelson, M.T., H. Cheng, M. Rupart, L.F. Santana, A.D. Bonev, H.J. Knot, and W.J. Lederer. 1995. Relaxation of arterial smooth muscle by calcium sparks. *Science (Wash. DC).* 270:633–636.

Nicholas, W.L. 1984. The Biology of Free Living Nematodes. Clarendon Press, Oxford. pp. 31–53.

O'Brien, J., G. Meissner, and B. Block. 1993. The fastest contracting muscles of nonmammalian vertebrates express only one isoform of the ryanodine receptor. *Biophys. J.* 65:2418–2427.

O'Brien, J., H.H. Valdiva, and B. Block. 1995. Physiological differences between the α and β ryanodine receptors of fish skeletal muscle. *Biophys. J.* 68: 417–482.

Otani, H., H. Otani, and D. Das. 1988. α-Adrenoceptor-mediated phosphoinositide breakdown and inotropic response in rat left ventricular papillary muscles. *Circ. Res.* 62:8–17.

Otsu, K., H.F. Willard, V.K. Khanna, F. Zorzato, N.M. Green, and D.H. MacLennan. 1990. Molecular cloning of cDNA encoding the Ca²⁺ release channel (Ryanodine Receptor) of rabbit cardiac muscle sarcoplasmic reticulum. *J. Biol. Chem.* 265:13472–13483.

Oyamada, H., T. Murayama, T. Takagi, M. Iino, N. Iwabe, T. Miyata, Y. Ogawa, and M. Endo. 1994. Primary structure and distribution of ryanodine-binding protein isoforms of the bullfrog skeletal muscle. *J. Biol. Chem.* 269: 17206–17214.

Percival, A.L., A.J. Williams, J.L. Kenyon, M.M. Grinsell, J.A. Airey, and J.L. Sutko. 1994. Chicken skeletal muscle ryanodine receptor isoforms: ion channel properties. *Biophys. J.* 67:1834–1850.

Radermacher, M., V. Rao, R. Grassucci, J. Frank, A.P. Timerman, S. Fleisher, and T. Wagenknecht. 1994. Cryo-electron microscopy and three-dimensional reconstruction of the calcium release channel/ryanodine receptor from skeletal muscle. *J. Cell Biol.* 127:411–423.

Rios, E., J. Ma, and A. Gonzalez. 1991. The mechanical hypothesis of excitation-contraction (EC) coupling in skeletal muscle. *J. Mus. Res. Cell Motil.* 12: 127–135.

Rushforth, A., and P. Anderson. 1996. Splicing removes the *Caenorhabditis elegans* transposon Tc1 from most mutant Pre-mRNAs. *Mol. Cell. Biol.* 16:422–429.

Rushforth, A.M., B. Saari, and P. Anderson. 1993. Site-selected insertion of the transposon Tc1 into a *Caenorhabditis elegans* myosin light chain gene. *Mol. Cell. Biol.* 13:902–910.

Sakube, Y., H. Ando, and H. Kagawa. 1993. Cloning and mapping of a ryanodine receptor homolog gene of *Caenorhabditis elegans. Ann. NY Acad. Sci.* 707:540–545.

Somlyo, A.P., and A.V. Somlyo. 1994. Signal transduction and regulation in smooth muscle. *Nature (Lond.).* 372:231–236.

Takeshima, H., M. Iino, H. Takekura, M. Nishi, J. Kuno, O. Minowa, H. Takano, and T. Noda. 1994a. Excitation-contraction uncoupling and muscular degeneration in mice lacking functional skeletal muscle ryanodine-receptor gene. *Nature (Lond.).* 369:556–559.

Takeshima, H., M. Nishi, N. Iwabe, T. Miyata, T. Hosoya, I. Masai, and Y. Hotta. 1994b. Isolation and characterization of a gene for a ryanodine receptor/calcium release channel in *Drosophila melanogaster. FEBS Lett.* 337:81–87.

Takeshima, H., S. Nishimura, T. Matsumoto, H. Ishida, K. Kangawa, N. Minamino, H. Matsuo, M. Ueda, M. Hanaoka, T. Hirose, and S. Numa. 1989. Primary structure and expression from complementary DNA of skeletal muscle ryanodine receptor. *Nature (Lond.).* 339:439–445.

Takeshima, H., T. Yamazawa, T. Ikemoto, H. Takeura, M. Nishi, T. Noda, and M. Iino. 1995. Ca²⁺-induced Ca²⁺-release in myocytes from dyspedic mice lacking the type-1 ryanodine receptor. *EMBO (Eur. Mol. Biol. Organ.) J.* 14: 2999–3006.

Varro, A., N. Negretti, S.B. Hester, and D.A. Eisner. 1993. An estimate of the calcium content of the sarcoplasmic reticulum in rat ventricular myocytes. *Pflügers Arch.* 423:158–160.

Walrond, J.P., I.S. Kass, A.O.W. Stretton, and J.E. Donmoyer. 1985. Identification of excitatory and inhibitory motorneurons in the nematode *Ascaris* by electrophysiological techniques. *J. Neurosci.* 5:1–8.

Waterston, R., C. Martin, M. Craxton, C. Huynh, C. Coulson, L. Hillier, R. Durbin, P. Green, R. Shownkeen, N. Halloran et al. 1992. A survey of expressed genes in *Caenorhabditis elegans. Nature Genet.* 1:114–123.

Weisblat, D.A., L. Byerly, and R.L. Russell. 1976. Ionic mechanisms of electrical activity in somatic muscle of the nematode *Ascaris lumbricoides. J. Comp. Physiol.* 111:93–113.

Williams, B.D., B. Schrank, C. Huynh, R. Shownkeen, and R.H. Waterston. 1992. A genetic mapping system in *Caenorhabditis elegans* based on polymorphic sequence-tagged sites. *Genetics.* 131:609–624.

Wood, W.B. 1988. The nematode *Caenhorhabditis elegans.* Cold Spring Harbor Laboratory, Cold Spring Harbor, NY. pp. 1–16, 281–336.

Yano, M., R. El-Hayek, and N. Ikemoto. 1995. Conformational changes in the junctional foot protein/Ca²⁺ release channel mediate depolarization-induced Ca²⁺ release from sarcoplasmic reticulum. *J. Biol. Chem.* 270:3017–3021.

Zwaal, R.R., A. Broeks, J. van Meurs, J. Groenen, and R.H.A. PLasterk. 1993. Target-selected gene inactivation in *Caenorhabditis elegans* by using a frozen transposon insertion mutant bank. *Proc. Natl. Acad. Sci. USA.* 90:7431–7435.